COO-2522-6
CONF-760829--45

Applied Superconductivity Conference
Palo Alto 1976
Paper J1 - Final Version

PROGRESS TOWARD A PRACTICAL Nb-Ge CONDUCTOR*

A. I. Braginski, J. R. Gavaler, G. W. Roland,
Michael R. Daniel, M. A. Janocko, and A. T. Santhanam**

ABSTRACT

Properties of high-T_c Nb-Ge films deposited by sputtering and by chemical vapor deposition (CVD) have been investigated. Results of sputtering in the presence of controlled levels of O_2, N_2, Si, and of reactive sputtering in Ar-GeH_4, suggest that the high-T_c A15 phase is impurity- or defect-stabilized. In CVD deposits two tetragonal modifications were found: σ and T2, the latter probably stabilized by Cl_2. High critical current densities, J_c (H, T) of fine-grained sputtered films are attributed to flux pinning on A15 grain boundaries. In coarse-grained CVD films high self-field J_c's, 10^6 to 10^7 A cm^{-2} at T = 4.2 K, are attributed to pinning on dispersed σ-phase. Comparably high J_c's were also obtained in CVD A15 films doped with impurities. Low field ac losses p (H, T) were correlated with J_c and coating geometries. The feasibility of fabricating multifilamentary composite conductors by CVD was demonstrated experimentally and a fabrication process for long Nb_3Ge CVD tapes is being developed.

I. INTRODUCTION

The purpose of this paper is to review the progress in the study and development of the Nb_3Ge superconductor as accomplished by our group since the 1974 Applied Superconductivity Conference. We address the phenomenology of the high critical temperature A15 phase, and the characterization and understanding of the superconductor properties which are relevant for potential applications. On this basis we briefly characterize the status of our work aimed at fabricating practical Nb_3Ge conductors.

To synthesize Nb_3Ge we are using two methods: low energy sputtering[1,2] and chemical vapor deposition (CVD).[3,4] The first is being used primarily as an investigation tool, while the second is being developed as a process leading to conductor fabrication. The details of these synthesis methods were given previously.[1-4] In this paper we compare the behavior and properties of sputtered and CVD films.

The paper encompasses work performed under several programs and includes contributions of many individuals. By necessity, we present a rather general overview and refer the reader to more specific publications.

II. THE HIGH CRITICAL TEMPERATURE A15 Nb-Ge PHASE

Composition and Stability

The cell edge, a_o, of the A15 phase has been determined by x-ray diffractometer in the case of films sputtered on sapphire or alumina, and by powder camera for CVD layers removed from the substrate. The a_o range is typically 5.14 to 5.18 Å. Using the previously-determined curve for cell edge versus A15 composition,[5] this range in cell size would correspond to a compositional variation from nearly stoichiometric Nb_3Ge (∿ 25 at.% Ge) to a Ge-deficient phase containing about 14 at.% Ge. It is well verified that at high temperatures the solid solution limits of the A15 phase do not reach the ideal 3:1 ratio; at ∿ 1600°C, for example, the homogeneity limits are reported[6] as $NbGe_{0.15 \pm 0.01}$ (13 at.% Ge) and $NbGe_{0.22 \pm 0.01}$ (18 at.% Ge). There are no data on the solubility limits as a function of temperature below 1600°C, although the position of the Ge-rich boundary assumes considerable importance since it has generally been believed that the highest critical temperature, T_c, for any A15 compound will occur in the ordered stoichiometric phase. If the phase stability situation as related to T_c is considered for the series of Nb_3X compounds, where X = Sn, Al, Ga, or Ge, it is evident that there are two trends operative: As the size of the X-atom decreases (in the order listed), the T_c of the ordered stoichiometric A15 phase becomes higher. At the same time, however, this high-T_c phase becomes increasingly more difficult to prepare. In the Nb-Ge system, attempts to grow the high-T_c stoichiometric A15 phase from the melt are not successful. In fact, high T_c A15 material is not obtained at a deposition temperature, T_d, much greater than 1000°C.

There are three possible explanations for the occurrence of stoichiometric, or nearly stoichiometric, Nb_3Ge in A15-films: (1) a stoichiometric Nb_3Ge phase (25 at.% Ge) is thermodynamically stable at T ≤ 1000°C, (2) the Nb_3Ge (25 at.% Ge) is a thermodynamically metastable phase when deposited in the same temperature range, or (3) impurity stabilization results in deposition of high-T_c Nb_3Ge which otherwise cannot be obtained in the pure Nb-Ge chemical system. The conditions under which Nb-Ge is formed by low energy sputtering, CVD, or evaporation differ in at least two essential ways from those present when using ordinary bulk melting methods. First, the temperature of formation is low compared to the melting temperature, thus phases which are stable only at lower temperatures can be prepared. Second, the planar geometry of the deposition process is more favorable than the bulk geometry of melting for the accidental or deliberate introduction of impurities into the growing film.

X-ray and T_c data on sputtered films, which were grown in the presence of controlled levels of impurities, indicate that the high-T_c phase is impurity stabilized. These data[7] show that the three impurity elements which were investigated (oxygen, nitrogen, or silicon) are each capable of acting as the stabilizing agent. Nb-Ge films were also sputtered under conditions designed to minimize or eliminate residual gas contamination. This was done by sputtering Nb in an argon-germane (GeH_4) atmosphere in which the germane pressure was adjusted to deposit stoichiometric Nb_3Ge. Using otherwise optimum conditions, films were sputtered which had the Nb body-centered cubic structure with a greatly contracted cell edge of 3.25 Å whereas the normal cell edge for Nb is 3.31 Å. This result indicates that without the presence of impurities an Nb-Ge solid solution is formed which contains a substantial amount of Ge. According to the Nb-Ge phase diagram which was constructed from bulk data, the equilibrium solubility of germanium in niobium is less than 5% at all temperatures.

A detailed study of the possible impurity stabilization of the A15 phase in CVD films has not been done, but analytical data indicate that, if it does occur, the amount of impurity is small. We examined several of our films using an x-ray analyzer (EDAX) attachment to a scanning electron microscope but were unable to detect any metallic elements other than Nb and Ge in the films, except at the Hastelloy substrate-film interface where a diffusion layer is present. The detection limit of the EDAX unit is ∿ 1 wt.%. A spark source mass spectroscope analysis of a pure A15-phase film grown at 900°C showed Cl < 0.0120, Si ≲ 0.005, Al < 0.0005 at.% [illegible] vacuum

Manuscript received August 17, 1976.

*Review of programs supported by: AFOSR Contract No. F44620-74-C-0042 (in part); ERDA Contract No. E(11-1)-2522; NASA Contract No. NAS 3-20233. Part of this work was done at the Francis Bitter National Magnet Laboratory supported at MIT by NSF.

**Westinghouse Research Laboratories, Pittsburgh, PA 15235

DISCLAIMER

fusion analyses for oxygen in Nb_3Ge powders removed from the Hastelloy substrate showed oxygen contents from 0.67 wt.% (6.7 at.%) to 1.28 wt.% (12.5 at.%) with an average of 12 samples of 0.85 wt.% (8.6 at.%). This oxygen is, however, probably a result of the acid treatment used to remove films from Hastelloy, because Auger analyses of films on Hastelloy always showed less than 0.1 at.% O_2 (the detection limit).

There is evidence that at least one Nb-Ge phase, a tetragonal (T2) phase with $a \simeq 6.63$, $c = 11.96$ Å is impurity stabilized in the CVD process. This phase contains about 33 at.% Ge, i.e., it has essentially the same composition as the more usually encountered Nb_5Ge_3 σ phase, but has a different structure.[5] The occurrence of the T2 phase rather than σ Nb_5Ge_3 is a function of CVD parameters as shown in Fig. 1. It is favored by low temperature and/or low H_2 content in the gas phase.

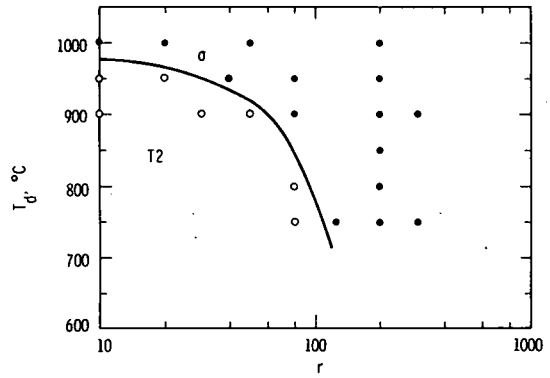

Fig. 1. Tetragonal phase occurrence vs. deposition temperature, T_d, and hydrogen to chloride ratio, r; o-T2 tetragonal phase present, •-σ-tetragonal phase present.

We define the H_2 content by the value of the molar ratio $r = H_2/(NbCl_4 + GeCl_2)$. Spark-source mass spectroscopy analyses showed high contents of Cl_2 in T2-containing samples, e.g., a sample of T2 prepared at 900°C in conditions r = 10 contained 20.0 at.% of Cl_2 as compared to a content of 0.19 at.% in a σ phase sample prepared at 900°C but with $r \gtrsim 300$. A marked, but less striking, difference was observed also for samples prepared at 800°C: 1.6 at.% Cl_2 in T2 prepared at r = 80 vs. less than 0.2 at.% Cl_2 in σ phase prepared at r = 200. Some of the chloride content of the chloride-rich samples is undoubtedly due to included unreduced niobium or germanium chlorides; nevertheless, T2 samples always contained at least twice the amount of Cl_2 as A15 samples prepared under the same T_d and r conditions (but different Nb/Ge gas ratio) or σ samples prepared at the same T_d but higher r.

Critical Temperature

Critical temperatures were measured by the standard four-point resistive method and by the inductive (susceptibility) method at 17 Hz. Also, linear extrapolation of upper critical field H_{c2} (T) has been employed at liquid hydrogen temperatures. The temperature measurement accuracy was ± 0.05 K for precise measurements and ± 0.2 K for routine characterization. The width of the Nb_3Ge superconducting transition was often as narrow as $\Delta T = 0.4$ to 0.7 K. More typically, however, it was of the order of $\Delta T = 1$ to 2 K especially in CVD films. This suggests the existence of compositional inhomogeneity in the A15 phase.

Both sputtering and CVD resulted in critical temperature onsets approaching 23 K. The question whether further enhancement of T_c would be achieved by improved atomic ordering was addressed by Blaugher.[8] Low-temperature annealing of CVD samples resulted in a measurable increase of the T_c onset. However, no direct measurements of the order parameter were performed due to the similarity of the x-ray atomic scattering factors for Nb and Ge. For as-deposited sputtered samples, onsets in excess of 22 K were recorded for a relatively wide range of T_d, 750 to 1000°C, in agreement with the results of Sweedler et al.[9] Below 900°C the critical temperature of CVD samples decreased with T_d as shown in Fig. 2. This decrease might be caused by the incorporation of unreduced Nb chlorides.

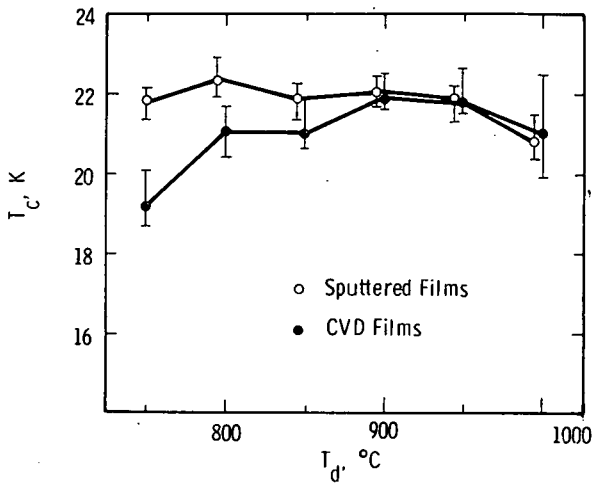

Fig. 2. Highest transition temperature, T_c, achieved for sputtered and CVD films versus deposition temperature, T_d. Bars indicate width of superconducting transition.

The highest T_c's were observed in single phase (A15) sputtered and CVD samples having a_o between ∿ 5.14 and 5.17 Å. This indicated Ge-concentrations in the range from nearly 25 at.% down to only 16 at.%. Insufficient accuracy of our analytical techniques prevented a precise determination of sample composition independent of the x-ray diffraction data.

Since Ge-deficiency implies disorder and a correspondingly degraded critical temperature, we believed initially that compositional inhomogeneity in the A15 phase is responsible for the high-temperature "filamentary" superconductivity. However, on the basis of good agreement between resistive and inductive (susceptibility) T_c measurements, and in the light of preliminary low temperature specific heat measurements,[10] we now admit the possibility that an A15 solid solution somewhat off stoichiometry can indeed have high T_c, perhaps due to a not-yet-understood defect ordering process. We hope that additional specific heat measurements will eventually resolve the question.

III. CRITICAL FIELDS, CURRENTS AND AC LOSSES

Upper Critical Field

The upper critical fields, H_{c2}, of Nb_3Ge samples prepared by sputtering and CVD in a variety of conditions, and covering a T_c range between 17 and 22.5 K, have been determined between 14 and 20 K. The H_{c2} values at 0 K have been calculated from dH_{c2}/dT at $T \to T_c$[11] using 90% of normal state resistivity, ρ_n, as a criterion for defining H_{c2} at a temperature T. Figure 3 presents the H_{c2} (0) data vs. T_c and indicates that the

highest-T_c sputtered films have higher H_{c2} than the CVD samples. Since the superconducting transitions of the latter are broader, their 90% ρ_n T_c's are somewhat lower. This is not sufficient, however, to account for the H_{c2} difference.

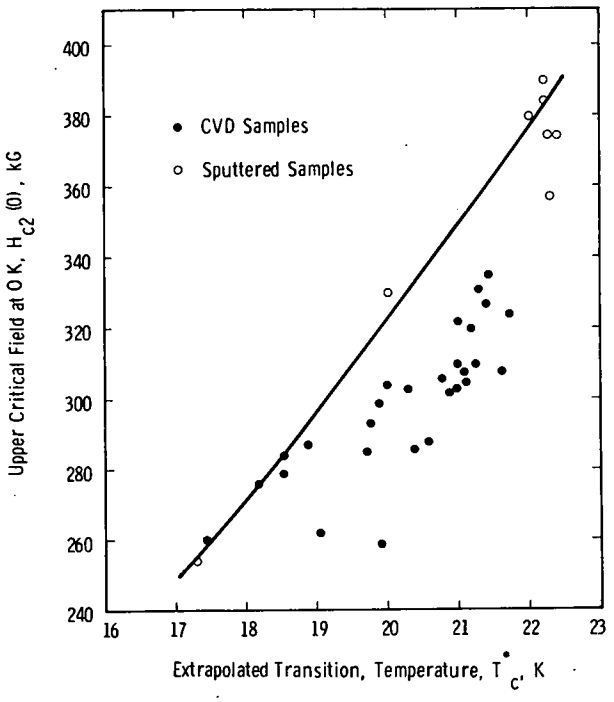

Fig. 3. Upper critical field at 0 K vs. transition temperature, T_c^* extrapolated from dH_{c2}/dT. Field applied perpendicular to the film plane. The H_{c2} (T_c^*) curve represents Usui's relation.[12]

Measurements show that the low temperature resistivity of sputtered fine-grained samples, $\rho_{25} \simeq 100$ to 150 μΩcm, is always substantially higher than that of CVD coarse-grained samples, $\rho_{25} \simeq 40$ to 60 μΩcm, independent of the deposition conditions. If $H_{c2} \propto \gamma\rho T_c$ where γ is the specific heat coefficient, then we can infer that the difference in ρ defined by the microstructure is more significant than ρ and γ variations with composition, defect concentration, etc., resulting from various deposition conditions. The scatter of H_{c2} (T_c) data reflects these variations. It can be noted that the trend of H_{c2} (T) data is approximated by the empirical H_{c2} (T_c) relation of Usui.[12] The results of Fig. 3 imply that for very high field applications sputtered Nb_3Ge may be preferred over the CVD material unless the resistivity of the latter is enhanced, e.g., by a modification of microstructure. However, even the present H_{c2} level of CVD materials should be adequate for applications up to the 200 kilogauss level.

Critical Current Density and Microstructure

The critical current densities, J_c, have been determined from magnetization[13] and transport measurements of small samples in fields ranging from zero up to 200 kilogauss at 4.2 K, and in a narrower field range between 4.2 K and the critical temperature. Our earlier results[4,14,15] and those of other authors[16-18] demonstrated that Nb_3Ge films, prepared by various methods, can support high critical current densities in a broad range of fields and temperatures. Our main interest here is to compare J_c characteristics of sputtered and CVD samples. Previous comparison of high field J_c's with the field, $H_\perp$, perpendicular to the film plane, indicated that sputtered films exhibit J_c's at least an order of magnitude higher than those of CVD layers. Assuming that flux pinning in Nb_3Ge occurs primarily on grain boundaries we attributed the above result to differences in microstructure.[15] Grain size estimates, based on scanning electron microscopy (SEM) of fractured films, indicated that CVD layers have coarse columnar grains from several thousand angstroms up to above 1 μm in diameter whereas grains in the 1000 Å range are typical of sputtered Nb_3Ge. Recent microstructure studies by transmission electron microscopy (TEM) generally confirm the SEM observations. The grain size dependence upon T_d in the range from 750 to 1000°C is significant but insufficient to offset the difference. Two examples of CVD sample microstructure are shown in Fig. 4.

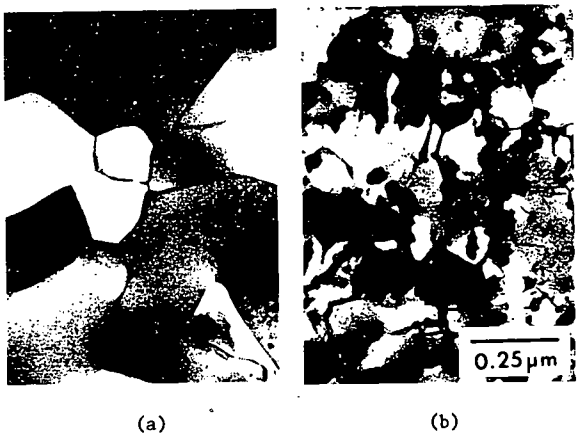

Fig. 4. TEM micrographs of (a) single phase A15, T_d = 950°C, and (b) A15 + σ, T_d = 900°C. Small grains in (b) are the σ-phase precipitates.

The proposed correlation of J_c with microstructure, although plausible, cannot explain why some CVD samples exhibit at 4.2 K high critical current densities, 5 x 10^6 to 10^7 A cm^{-2} in zero field, and ∿ 1 x 10^6 A cm^{-2} in $H_\perp$ = 50 kG, in spite of the large grain size. A more detailed study of CVD films revealed that in a wide field range the critical current densities depend upon the concentration and dispersion of the tetragonal σ-phase, Nb_5Ge_3, present in some deposits.[19] Pure, single phase A15 layers exhibit relatively low J_c's, while the presence of several volume percent of Nb_5Ge_3 results in J_c up to one order of magnitude higher, as shown in Fig. 5 which compares the J_c (H) characteristics at 4.2 K. However, with further increasing σ-concentration, the critical current density decreases sharply, probably due to internal strains and discontinuities in the A15 matrix. The critical temperature of σ-rich layers is also depressed. An example of J_c dependence upon the σ-phase concentration is shown in Fig. 6. The upper limit to the σ-phase concentration shown in the figure was estimated from Debye-Scherrer powder patterns. Only most recently the first TEM determination of σ concentration was achieved indicating satisfactory agreement with x-ray results. In a sample containing 10 ± 5 vol.% of σ (measured by x-rays) TEM indicates 9 to 11%. The Nb_5Ge_3 particles have a mean size of 600 Å with a mean spacing of 1600 Å. It is not yet known how the σ dispersion depends upon its concentration and the deposition conditions. Since the mean size and spacing of σ precipitates should affect J_c, the "optimum" σ-concentration of 5 ± 2 vol.% at the J_c peak in Fig. 6 may be rather accidental. Nonetheless, the peak reflects a trade-off between the enhanced flux

pinning and strain or defect level introduced by the σ-phase.

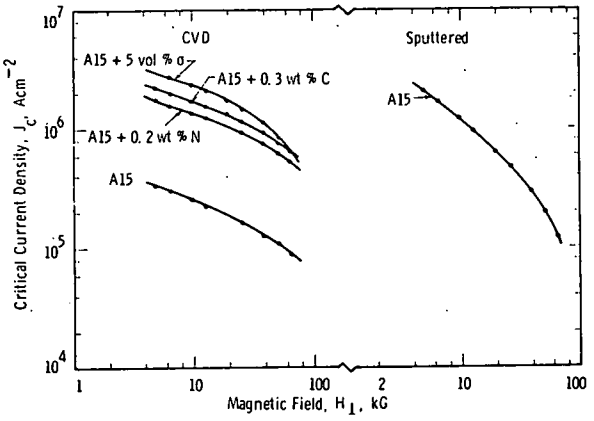

Fig. 5. Critical current density at 4.2 K vs. the perpendicular magnetic field intensity, $H_\perp$, for CVD and sputtered films. Results derived from magnetization measurements.

In the case of CVD layers the high critical current densities can be obtained not only by σ-doping but also by introducing impurities. In analogy to earlier studies of Nb_3Sn[20,21] we have used nitrogen, CO_2 and C_2H_6 doping to enhance flux pinning in single-phase A15 deposits. Various doping methods result in comparable critical current densities, as shown in Fig. 5. The critical temperatures of doped, high-J_c samples are depressed by 1 to 4 K compared to the T_c of a pure A15 phase. The most detrimental to T_c and least effective is doping with CO_2. Results of the impurity-doping study will be reported and discussed elsewhere.[22]

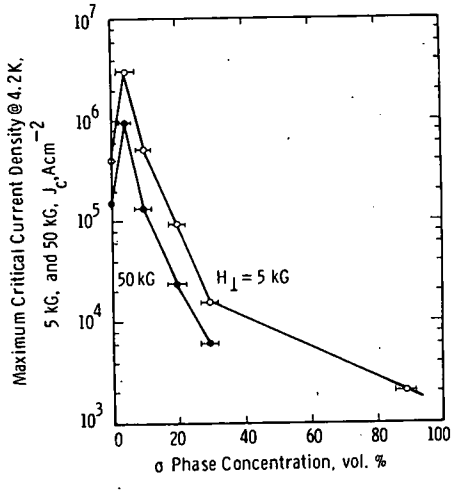

Fig. 6. Maximum achieved critical current density vs. the upper limit of σ-phase concentration.

Comparison with sputtered samples shows that in the low and moderate field range, below 100 kilogauss, similar levels of J_c's can be achieved in coarse-grained σ- or impurity-doped Nb_3Ge prepared by CVD, and in single A15 phase sputtered films which are fine grained. Indeed, we have no evidence of any further J_c enhancement due to the presence of σ-phase in sputtered samples. This indicates that in sputtered films flux pinning occurs predominantly on grain boundaries, as anticipated earlier.[15]

At very high fields and at temperatures near T_c, the J_c's of sputtered films exceed those of CVD layers. The early figure of $J_c = 10^5$ A cm^{-2} at 200 kilogauss, 4.2 K[14] for a thin (< 1 μm) sputtered sample still remains unsurpassed. For CVD layers the extrapolation from lower field J_c data to 200 kG, 4.2 K, (by using the scaling laws,[23] and available H_{c2} values) gives J_c's of approximately 5 x 10^4 A cm^{-2}. The direct resistive measurement of small, but relatively thick (5 to 10 μm), CVD samples is difficult due to high measuring currents, and resulting heating effects. Based on the extrapolation we believe that sputtered samples have higher J_c's due to their better uniformity and higher H_{c2} values discussed above. Improvements in high field properties of CVD materials are feasible.

The temperature dependence, J_c (T), of Nb_3Ge has been determined in the low and moderate field range, up to 65 kilogauss. At self- and low-fields it can be approximated by

$$J_c(t) = J_c(1 - t^2)^m \qquad (1)$$

where $t = T/T_c$ is the reduced temperature, and $m \simeq 1 - 4$.[24] With increasing field the functional dependence gradually changes, and becomes more linear with a pronounced tail. The relevant segment of the JHT surface can be expressed by (1) with m becoming an increasing function of H. Reduced J_c (t) curves for $H_\perp$ equal 5 and 50 kG with $m \simeq 4$ and 6 are shown in Fig. 7. We suspect that the m ($H_\perp$) scatter is due to inhomogeneity of the A15 phase.

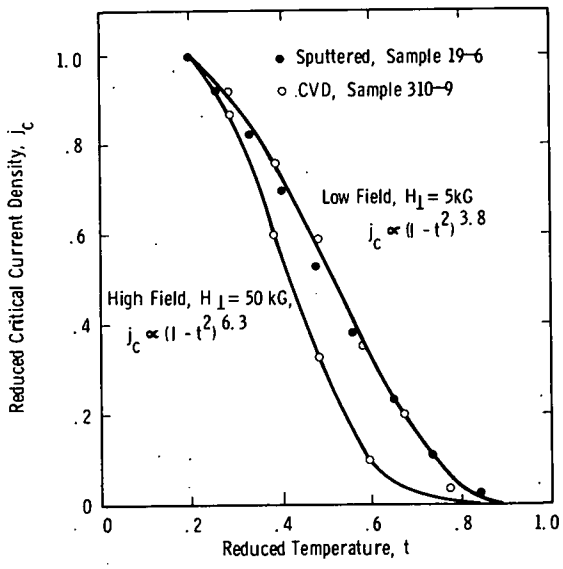

Fig. 7. Reduced critical current density vs. reduced temperature for sputtered and CVD films at $H_\perp$ = 5 and 10 kG. The J_c values are derived from magnetization measurements.

What are the ultimate upper limits to J_c (H, T) of Nb_3Ge, and what are the advantages over Nb_3Sn or V_3Ga? Assuming the plastic flux lattice shear mechanism,[23] with $H_{c2} \simeq 380$ kG and J_c (200 kG) = 10^5 A cm^{-2}, one obtains at 4.2 K, in low fields, J_c of the order of 10^7 A cm^{-2}, but even higher values are projected for Nb_3Sn and V_3Ga.[25] The J_c's of Nb_3Ge win out either at very high fields (≥ 200 kG) or at high temperatures, above 10 to 14 K.

Losses

The ac losses in a given superconductor depend, among other factors, upon its shape and configuration with respect to the external field. Thus far, we have investigated only planar Nb_3Ge CVD films deposited on one side of short (2.5 to 5 cm) sections of Hastelloy B ribbon, typically 1.3 cm or 0.6 cm wide. Such tapes can be envisaged for application in superconducting power transmission lines (SPTL). We measured 60 Hz surface current losses with $H_{||}$ in plane conforming to the geometry of Bean's model of the critical state.[26] The samples were too short to permit loss measurements in a hairpin or shorted-turn sample configuration where the flux is excluded from the substrate. Hence, we used the short sample technique,[27] and our loss data included the hysteretic and eddy-current contribution of the substrate, as well as losses originating at the substrate/superconductor interface where a non-uniform diffusion layer exists, as mentioned before.

The 60 Hz loss p (H, T) measurements have been performed using an electronic low power factor wattmeter.[28] Standard measurements were performed at 4.2 K, but p (T) characteristics were also determined. Losses in high-J_c samples, doped with σ-phase or gas impurities, conform well to the Bean's model, $p \sim H_{||}^{n}$, with $n \gtrsim 3$, since J_c is not too field-dependent. A typical p (H) dependence is shown in Fig. 8a for a σ-doped sample. For samples with sufficient flux pinning, losses scale well with $1/J_c$, i.e., J_c calculated from loss data at a peak field of ∿ 2 kilogauss agree well with those obtained from static, magnetization measurements. For such samples one observes:

$$p(t) \sim (1 - t^2)^{-m} \qquad (2)$$

or a less steep loss increase with temperature up to t = 0.6 - 0.9, depending upon the material uniformity.

In pure A15 samples with a low level of flux pinning, and steep J ($H_{||}$) dependence, losses increase dramatically with H such that n = 4 to 6 up to the region of flux penetration between $H_{||}$ = 1000 and 2000 gauss (peak) where n → 1 as shown in Fig. 8b. In such samples losses increase very gradually with temperature, or even decrease at higher fields. The A15 samples with significant Ge-deficiency exhibit n < 3 (Fig. 8c) from very low fields up, suggesting easy flux penetration due to the material non-uniformity.

In all the above results a surface field barrier, ΔH, evidenced by very low losses at H < ΔH, could not be observed.

Thompson et al. demonstrated recently that Nb_3Ge losses in the Kim tube geometry can be extremely low after an appropriate treatment of the tube surface.[29] Proper surface topography and pinning seem to greatly enhance the surface field barrier as shown by Bussière et al. for Nb_3Sn tubes.[30] Tubes of both materials show 60 Hz losses at 4.2 K as low as $p \leq 1\ \mu W/cm^2$ for a surface current σ = 500 A/cm, while the SPTL requirements allow up to 10 $\mu W/cm^2$. For our sample geometry we were not in a position to observe the surface barrier even in samples with sufficient flux pinning since losses at σ ≤ 500 A/cm were dominated by the diffusion layer and Hastelloy substrate contributions (Hastelloy alone contributes 10 to 15 $\mu W/cm^2$ at 500 A/cm). The losses at 500 A/cm, rms were typically in the range of 30 to 100 $\mu W/cm^2$, depending upon the J_c value and the deposition temperature. From loss data for Nb_3Ge deposited on various metallic substrates (Nb, Hastelloy, stainless steel and copper), and after Nb_3Ge surface treatment analogous to that of Refs. 29 and 30 we concluded that the dominant loss component is that of the superconducting diffusion layer. In the case of Hastelloy the layer forms by diffusion of nickel into Nb_3Ge, and is up to 1 μm thick as revealed by Auger spectroscopy.[31] The diffusion of copper from Cu substrates is even more pronounced. To properly measure surface current losses on short samples a different geometry of coating is required. The Nb_3Ge layer should be deposited on all substrate surfaces, and around the edges, to approximate the Kim tube situation, and permit flux exclusion from the diffusion region and the substrate. This tape geometry is also necessary for the double helix SPTL cable where the magnetic field is present on both sides of the tape. Development of such tape conductor represents one of our present goals.

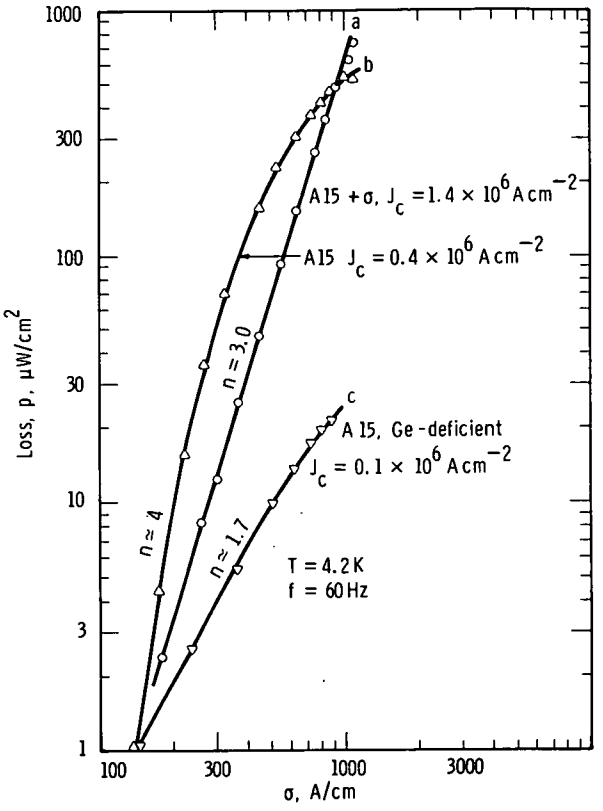

Fig. 8. Low frequency losses at 4.2 K vs. rms surface current density calculated from field intensity. Comparison of CVD samples of different composition and flux pinning level. The J_c values @ 5 kG were obtained from dc magnetization measurements.

IV. PROGRESS TOWARDS A PRACTICAL CONDUCTOR

Composite Tape Conductors

Tapes of Nb_3Ge can find application in SPTL at temperatures up to 14 to 16 K and in high field dc magnets producing fields in the range of 200 to 250 kilogauss. The planar tape configuration is best suited for superconductor deposition from a vapor phase. Flexible, high strength metallic ribbon is used as a substrate. Its thermal expansion coefficient β should exceed that of Nb_3Ge ($\beta \gtrsim 7.7 \times 10^{-6}$/°C in the 20 to 760°C temperature range[5]), so that the superconductor would be in compression. Coating of equal thickness should be applied to both surfaces to avoid ribbon deformation. For applications such as the double helix SPTL cable, the superconductor should enclose the ribbon entirely. The outer surfaces of Nb_3Ge should be coated by flux jump stabilizing layers of copper having a high resistance ratio. We have previously fabricated[4] short tape sections, up to 30 cm in length with Nb-Ge layers 2 to 5 μm thick, grown by CVD on one side of 1.27 cm wide, stationary Hastelloy B ribbon substrate ($\beta \gtrsim 13 \times$

10^{-6}/°C). Flux-jump stabilization was provided by first sputtering copper on the Nb_3Ge and then electroplating to final thickness. Superconducting properties of these tapes were reported.[4] Mechanical testing indicated bend radius values similar to Nb_3Sn tapes with a strain limit $\varepsilon > 0.2\%$.[32] Unfortunately, the tape sections exhibited marked longitudinal non-uniformity of thickness and composition caused by longitudinal gas-phase composition gradients in the CVD reactor tube. Hence, material characteristics reported here have been determined on short samples only. Recently we constructed a moving tape CVD system capable of producing lengths of tape, either one-, two-side, or around-the-edge-coated with the Nb_3Ge superconductor of acceptable uniformity. The system is analogous in principle to that developed by Hanak et al.[33] for producing Nb_3Sn tapes by CVD. Initial Nb_3Ge coating tests are now in progress. Cladding of Nb_3Ge will be achieved probably by E-beam evaporation of high resistance ratio copper. Firm adhesion to the Nb_3Ge surface has been already demonstrated.[34]

Filamentary Conductors

In the absence of metallurgical methods for processing multifilamentary Nb_3Ge, the use of CVD was proposed to form composite wire analogous to fiber reinforced structural composites.[35] In particular, alumina fiber reinforced composites, Al_2O_3/Al, could be contemplated since Al_2O_3 fibers offer a good thermal expansion match with Nb_3Ge and have very high longitudinal and transverse moduli (although low tensile strength). A 200 filament Al_2O_3 yarn (DuPont Fiber FP) with a filament diameter of 20 μm was coated with Nb_3Ge. Simultaneous coating of individual filaments was achieved with satisfactory uniformity as shown in Fig. 9. The Nb_3Ge filaments and filament bundles were

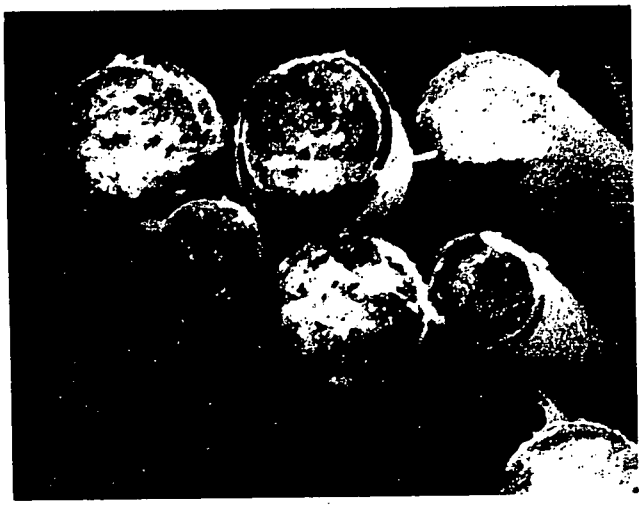

Fig. 9. SEM photograph of Nb_3Ge filaments formed by CVD on alumina yarn fibers 20 μm in diameter.

electroplated with copper to allow measurements of superconducting properties, and to insure wetting in the next processing step consisting of vacuum infiltration of liquid aluminum to form a composite wire. The filament critical temperature was 21 K with onset at 21.5 K. The upper strain limit figure indicates that a multifilamentary wire could be made with a twist pitch of the order of a few centimeters. Wires could then be cabled to achieve the desired current carrying capability. Approximate loss calculations suggest that such a type of conductor could be successfully used in Tokamak fusion reactors to produce high dc fields in the presence of superposed transverse and longitudinal pulsed fields since the dominant losses in the composite cable would be due to eddy currents in the normal matrix.[36]

Fabrication Methods

Assuming that fabrication of Nb_3Ge will be limited to low-temperature deposition from a vapor phase, it is desirable to define the preferred deposition method. Should it be a PVD (physical vapor deposition) or CVD? Thus far, high-T_c Nb_3Ge has been synthesized by low energy, low deposition rate sputtering, by E-beam evaporation,[16,37] and by CVD. Of these, CVD and E-beam evaporation are amenable to mass fabrication. Sputtering could also work if a high rate, low energy process such as magnetron sputtering were successfully developed for Nb_3Ge. The CVD process offers conductor geometry flexibility, especially in the case of filamentary deposition, and calls for the lowest capital investment, if performed at atmospheric pressure. It is, however, an inherently impure and complicated process. The control of the deposit microstructure is limited. E-beam evaporation offers the advantage of very high deposition rates, and it is cleaner, but the composition control is relatively difficult, and the deposit microstructure similar to that obtained by CVD. In both cases impurity doping or layering will probably be necessary to achieve high J_c's and low losses, thus resulting in some degradation of T_c and conductor uniformity. As shown above, the best results for small, thin Nb_3Ge samples especially at very high fields, have been achieved by low energy, low rate sputtering, without necessitating any doping or microstructure control. It is thus desirable to continue efforts aimed at developing high deposition rate sputtering of Nb_3Ge. Unless this is achieved, CVD will be the preferred method since it is already reaching a stage where fabrication of long conductors becomes possible. Eventually, sputtering may win out for planar conductors, while for filamentary wire fabrication CVD will be preferred.

Economics

Deposition from a vapor phase is usually more costly than metallurgical processing. Also, Ge is substantially more expensive than, for example, Sn. Cost estimates were made for mass production of Nb_3Ge tape using CVD on Hastelloy B substrates. Prior to the copper cladding (laminating) operation, the cost per unit tape length was found to be approximately 50% higher than for Nb_3Sn tape of identical dimensions. Assuming that in applications above a certain temperature, or field intensity, the current carrying capability of the conductor will exceed that of Nb_3Sn or V_3Ga by more than 50%, the cost per kA-unit length will become economically attractive.

With respect to the availability of raw materials, we note that the massive use of Ge would significantly exceed the present supply. A lead-time of several years would be required to open or reopen additional primary Ge sources. Such sources are, however, available up to the limit of the order of 100 to 200 metric tons a year.[38,39] For small scale applications such as high-field laboratory magnets, the present Ge supply is adequate.

CONCLUDING REMARK

The studies performed over the past two years advanced the characterization and understanding of Nb_3Ge material properties to the point where a practical conductor can be envisaged. The possibility of fabricating both tape and filamentary conductors exists. In the near term, tape conductors should first become available.

REFERENCES

1. J. R. Gavaler, Appl. Phys. Lett. 23, 480 (1973).
2. J. R. Gavaler, M. A. Janocko, and C. K. Jones, J. Appl. Phys. 45, 3009 (1974).
3. A. I. Braginski and G. W. Roland, Appl. Phys. Lett. 25, 762 (1974).

4. G. W. Roland and A. I. Braginski, Adv. Cryo. Eng. Vol. 22 (1976), in press.
5. A. I. Braginski, G. W. Roland, and Michael R. Daniel, Appl. Polymer Symp. No. 29, 93 (1976).
6. J. H. Carpenter, J. Phys. Chem. 67, 2141 (1963).
7. J. R. Gavaler, AIP Conf. Proc. - 2nd Conf. on Superconductivity in d- and f-Band Metals, 1976 (in press).
8. R. D. Blaugher (Westinghouse Research Labs) - unpublished results.
9. A. R. Sweedler, D. E. Cox, S. Moehlecke, R. H. Jones, L. R. Newkirk, and F. A. Valencia, J. Low Temp. Phys. 24, 5/6 (1976).
10. G. R. Stewart (Stanford University) - unpublished results.
11. N. R. Werthamer, E. Helfand, and P. C. Hohenberg, Phys. Rev. 147, 295 (1966).
12. N. Usui (Nihon University), Manuscript NUP-A-75-14.
13. Michael R. Daniel and M. Ashkin, Cryogenics, 1976 (in press).
14. J. R. Gavaler, Science 183, 293 (1974).
15. J. R. Gavaler, M. A. Janocko, A. I. Braginski, and G. W. Roland, IEEE Trans. MAG-11, 172 (1975).
16. Y. Tarutani, M. Kudo, and S. Tagushi, Proc. V Int. Cryo. Eng. Conf., Kyoto, (1974), p. 477.
17. R. J. Bartlett, H. L. Laquer, and R. D. Taylor, IEEE Trans. MAG-11, 405 (1975).
18. L. R. Testardi, Solid State Comm. 17, 871 (1975).
19. A. I. Braginski, Michael R. Daniel, and G. W. Roland, IEEE Trans. MAG-12 (1976), in press.
20. R. E. Enstrom and J. R. Appert, J. Appl. Phys. 43, 1915 (1972).
21. G. Ziegler, B. Blos, H. Diepers, and K. Wohlleben, Z. Ang. Phys. 31, 184 (1971).
22. G. W. Roland, Michael R. Daniel, A. I. Braginski, and A. T. Santhanam, AIME Symposium on Superconducting Materials and Applications IV, Niagara Falls, September 1976.
23. E. J. Kramer, J. Appl. Phys. 44, 1360 (1973), and J. Electronic Mat. 4, 839 (1975).
24. Michael R. Daniel, A. I. Braginski, G. W. Roland, J. R. Gavaler, R. J. Bartlett, and L. R. Newkirk, (submitted to J. Appl. Phys.).
25. Michael R. Daniel, to be published in Cryogenics.
26. C. P. Bean, Rev. Mod. Phys. 36, 31 (1964).
27. O. Horigami, J. F. Bussière, and Y. Tanaka, Cryogenics 15, 660 (1975).
28. Low power factor wattmeter Model IH744, constructed by the Brookhaven National Laboratory.
29. J. D. Thompson, M. P. Maley, L. R. Newkirk, and F. A. Valencia, Los Alamos Sci. Lab, preprint LA-UR 76-555.
30. J. F. Bussière and M. Suenaga, J. Appl. Phys. 47, 707 (1976).
31. J. Schreurs (Westinghouse Research Laboratories) - unpublished results.
32. C. J. Klamut (Brookhaven National Laboratory) - unpublished results.
33. J. J. Hanak, K. Strater, and G. W. Cullen, RCA Rev. 25, 342 (1964).
34. E. Adam (AIRCO) - private communication.
35. D. W. Deis (Westinghouse Research Labs, now at Lawrence Livermore Laboratory).
36. J. H. Murphy (Westinghouse Research Laboratories) - unpublished results.
37. A. B. Hallack, R. H. Hammond, and T. H. Geballe, Appl. Phys. Lett. 29, 314 (1976).
38. J. Adams (Eagle-Picher Ind.) - private communication.
39. H. R. Babitzke, Bureau of Mines Bull. 677 (1975).